AN ALGORITHM FOR 3D ULTRASOUND IMAGING

João M. Sanches and Jorge S. Marques

Instituto Superior Técnico and Instituto de Sistemas e Robótica
Torre Norte, Av. Rovisco Pais, 1049-001, Lisbon, Portugal

ABSTRACT

This paper describes an algorithm for the reconstruction of 3D medical objects from ultrasound images complemented with measurements of the sensor location. Reconstruction is performed by filtering and interpolating the available data using an optimal Bayesian criterion. The object is represented by a function, belonging to a finite dimension vector space and a Rayleigh model is adopted to describe the image formation process.

1. INTRODUCTION

Ultrasound techniques play a key role in medicine since they allow non invasive and non ionizing measurements of the organs geometry and motion [1]. To obtain an image an ultrasound beam is applied to the human body and the echo amplitude is measured and displayed. The ultrasound image is built by representing the received echos along different ray directions. Since all scanning rays belong to the same plane, each ultrasound image represents a cross section of the human body along an inspection plane. This scanning mode is denoted by B-mode scan. A current research goal is the use of ultrasound methods for 3D reconstruction and visualization of human tissues and organs [4, 5, 3]. Two difficulties have to be considered: image noise and the estimation of the sensor location. Ultrasound imaging has poor signal to noise ratio due to the presence of speckle noise (multiplicative noise) and due to the distortion introduced by the acquisition system. Sensor position is measured by an external device (e.g., an electromagnetic locator) but measurement errors can not be negleted since they degrade the reconstruction results.

This paper addresses the 3D reconstruction of medical objects from a set of ultrasound images representing cross sections of the body, taken from different positions and orientations. The images were obtained with a free-hand echographic equipment complemented with a spatial locator attached to the ultrasound probe, giving the current position and orientation of the scanning plane. The experimental set up is described in [8]. It is assumed in this paper that the sensor position and orientation are accurately known and therefore no measurement errors are considered. This is not always true. Location errors my produce significant misalignment of the inspection planes, degrading the reconstruction results. We have carefully selected image sequences where these errors are small. A Bayesian approach using a MAP criterion is adopted to reconstruct the 3D tissue information. The echo magnitude is modeled as a random variable with Rayleigh distribution [6, 7], suggested by the image formation process. A Gibbs distribution is used for incorporating the prior knowledge about the unknowns parameters [9, 11]. The prior improves the parameter estimation and introduces a regularization effect which helps the convergence of the estimation algorithm.

The estimation of the tissue properties inside a region of interest can be considered as an interpolation problem where an unknown function is estimated from a set of noisy and sparse observations. Not all points of the volume of interest are intersected by images planes. Therefore, it is necessary to fill the gaps. A second case can also occur. Some regions are sometaimes intersected by more than one plane. The corresponding images should therefore be combined to improve the estimates [2]. This operation is often denoted as spatial compounding [6, 12].

The proposed method is evaluated using synthetic and medical data.

2. PROBLEM DESCRIPTION

It will be assumed that the function f describing the acoustic properties of human tissues belongs to a class of admissible functions defined in a set, $\Omega \subset R^3$, i.e., $f : \Omega \rightarrow R$. Furthermore, it is assumed that the set of admissible functions is a finite dimension vector space $\mathbf{F}$ with known basis functions, $b_i : \Omega \rightarrow R$. Therefore, each function $f \in \mathbf{F}$ can be expressed as a linear combination of the basis functions,

$$f(x) = \sum_{i=1}^{N} b_i(x) u_i \tag{1}$$

where $u_1, u_2, ..., u_N$ are the coefficients to estimate. Using matrix notation, $f(x)$ can be written as follows:

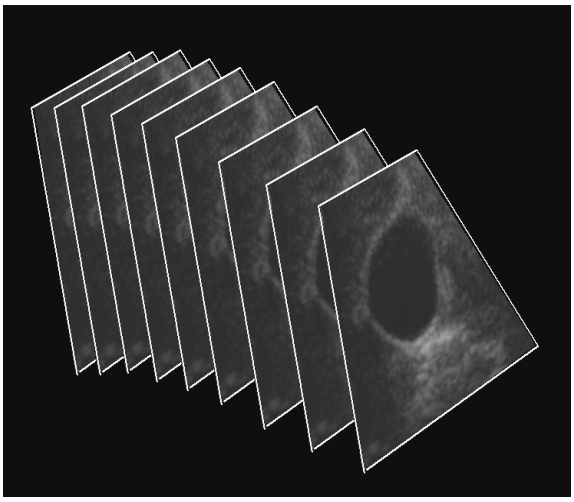

Figure 1: Scanning planes.

$$f(x) = B(x)^T U \tag{2}$$

where $B(x) = [b_1(x), b_2(x), ..., b_N(x)]^T$ is a vector of basis functions and $U = [u_1, u_2, ..., u_N]^T$ is a Nx1 vector of coefficients. The problem addressed in this paper can be stated as follows: we want to estimate $f(x)$, given a sequence of ultrasound images, with known sensor positions and orientations. This sequence is used to form a set of data points, $V = \{v_i\}$, with $v_i = (y_i, x_i)$, where y_i measures the reflexivity at location $x_i \in R^3$. It is assumed that each $b_i(x)$ is a local function obtained by shifting a known function $h : R^3 \rightarrow R$, i.e.,

$$b_i(x) = h(x - \mu_i) \tag{3}$$

where $\mu_i \in R^3$ is the i-th node of a 3D cubic grid (see Fig. 2) defined in Ω (the grid step is Δ), and $h(x)$ is a tri-linear interpolation function defined by:

$$h(x) = \begin{cases} \prod_{i=1}^{3} (1 - \frac{|x^i|}{\Delta}) & x \in \delta \\ 0 & \text{otherwise} \end{cases} \tag{4}$$

where x^i is the i-th coordinate of x and $\delta = [-\Delta, \Delta]^3$.

The grid defines a partition of Ω into cubic voxels. Each basis function has a finite support formed by 8 voxels and each 3D point belongs to 8 support regions (See Fig. 2). Therefore to compute $f(x_0)$ defined in (2) only 8 coefficients are needed since all other basis functions are zero at $x = x_0$. The estimation of the unknowns coefficients U, given a set of observations, V, can be formulated as a Bayesian estimation problem. Adopting the MAP[15] method this leads to the following optimization problem:

$$\hat{U} = arg \max_{U} \ln(p(Y|U)p(U)) \tag{5}$$

where $p(V|U)$ is obtained using the sensor model and p(U) is the prior. This formulation leads to a huge non convex optimization problem which will be solved using numeric methods [14].

2.1. Sensor Model

It is assumed that the observations consist of a set of 2D images obtained by intersecting the volume with non parallel plans defined by the sensor position and orientation (see Fig.1). Therefore, additional hypothesis must be made to estimate f in Ω.

There are three main sources of errors in this system: sensor position errors, tissue movement and deformation during data acquisition and intensity measurements errors. Only the third type of errors will be considered in this work. It will be assumed that the sensor orientation and location is accurately measured and that the observed organs do not move during the acquisition process. This is not true in general. Sensor position errors may cause significant misalignment of the cross sections. Organ motion and deformation is also a relevant issue. Recent research has addressed this problem in order to improve the robustness of the estimation process [13].

In this paper, pixel intensities are considered as realizations of independent random variables with Rayleigh distribution [6]. Statistical independence of all elements of Y is assumed because the point spread function of the acquisition system is smaller than the inter-pixel distance. Therefore, the likelihood function is given by

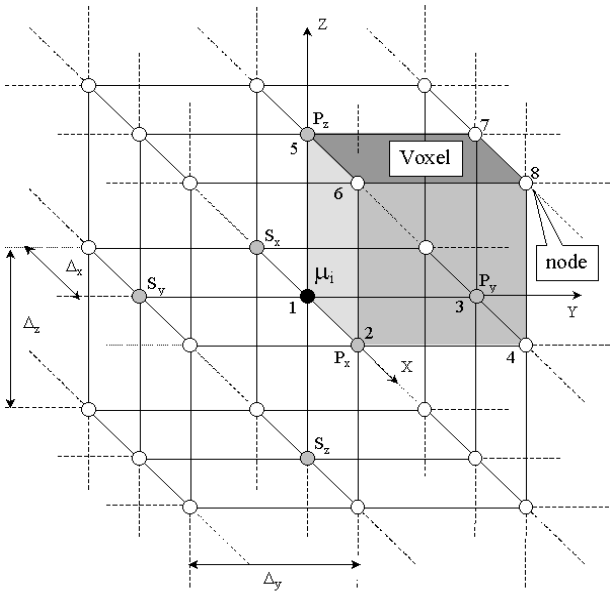

Figure 2: 3D grid of points.

$$p(Y|U) = \prod_i \frac{y_i}{f(x_i)} e^{-\frac{y_i^2}{2f(x_i)}} \tag{6}$$

where $f(x)$ is the mean intensity of the back scattered radiation at $x \in \Omega$. The parameter of the Rayleigh distribution is the mean square value of the amplitude of all sinusoids arriving at the sensor from each resolution cell.

2.2. Prior Model

Not all the U vectors occur with the same probability. The available knowledge about the spatial properties of human organs and tissues can be used to define a prior distribution. In this work, a Gibbs prior is adopted [9], based on a set of quadratic potential functions. The potential functions are used to guarantee the smoothness of the spatial coefficients. This introduces a regularization effect which allows to recover the unknown coefficients even when there is no data in a given region. In addition, regularization also improves the convergence of the optimization algorithm. The prior distribution used in this paper is given by

$$p(U) = \frac{1}{Z} e^{-\alpha \sum_{(i,j)\in\Gamma} P_i(u_j)} = \frac{1}{Z} e^{-\alpha \sum_{(i,j)\in\Gamma} (u_i - u_j)^2} \tag{7}$$

where Γ is the set of all pairs of grid indices (i, j) such that $\|x_i - x_j\| \leq \Delta, i \neq j$ (See Fig.2), and Z is a normalization factor. Each grid node is connected to 6 neighbors, except boundary nodes. The α parameter measures the strength of each connection. High values of α correspond to strong connections between neighboring nodes (differences receive a high penalty) while low values of α correspond to weak connections. It is often convenient to assume that α varies during the optimization process, starting with a high value which is gradually reduced.

3. PARAMETER ESTIMATION

Parameter estimation is performed using the MAP method. This leads to the maximization of the joint density p(Y,U) given by:

$$p(Y,U) = \prod_i [\frac{y_i}{f(x_i)} e^{-\frac{y_i^2}{2f(x_i)}}] \frac{1}{Z} e^{-\alpha \sum_{(i,j)} P_i(u_j)} \tag{8}$$

The maximization of $p(Y, U)$ with respect to U is a difficult problem since the number of parameters to estimate is very large (typically thousands of coefficients) and $p(Y, U)$ is a non convex function. Simpler expressions are obtained by maximizing $\ln p(Y, U)$,but the main difficulties remain.

Several methods are available to deal with large scale optimization problems, which fit in two broad categories: stochastic algorithms and deterministic algorithms. The ICM algorithm proposed by Besag is used in this paper [10]. The ICM

algorithm simplifies the optimization process by optimizing the objective function with respect to a single variable at a time, keeping the other variables constant[9]. Each step is a 1D optimization problem which can be solved in a number of ways. This step is repeated for all the unknown coefficients in each iteration of the ICM algorithm.

To optimize (8) with respect to a single coefficient u_p the following stationary condition must be met,

$$\frac{\partial}{\partial u_p} \ln p(Y/U) + \frac{\partial}{\partial u_p} \ln p(U) = 0 \tag{9}$$

Using the prior (7) and sensor model (6) the stationary condition is written as

$$u_p = \frac{1}{4\alpha N_v} \sum_i \frac{y_i^2 - 2f(x_i)}{f^2(x_i)} b_p(x_i) + \bar{u}_p \tag{10}$$

where $\bar{u}_p$ is the average value of the neighboring coefficients. This equation suggests an iterative procedure to compute $\hat{u}_p$, known as fixed point algorithm. Convergence is guaranteed if the right hand side is a contraction. In this paper, a single iteration is performed to update the unknown coefficient u_p in each iteration of the ICM algorithm.

4. EXPERIMENTAL RESULTS

The Rayleigh reconstruction algorithm was tested with synthetic and real data. Fig. 3 shows the results of a numerical test performed with synthetic data. The function to reconstruct is binary: it takes a value 0.75 in the interval $[-0.5, 0.5]^3$ and 0.25 outside. A grid of 101x101x101 nodes was used to approximate this function f in the interval $[-1, 1]^3$. The measurements used in this example consist of 50 images obtained by cutting f along non parallel planes and corrupting the cross sections with Rayleigh multiplicative noise, according to (6). Figs. 3a-d), show two cross sections of f and the synthetic images generated by the Rayleigh model. Figs. 3e-f) show the corresponding cross sections of the reconstructed function, $\hat{f}_r$. The SNR of the reconstructed function is 13.5 dB. Since the whole volume is estimated, it is possible to obtain new cross sections with arbitrary orientations. Figs. 3g-h) illustrate this operation by showing new cross sections obtained from the reconstructed volume. Fig. 3i-j) give an overall view of the reconstructed function visualized by ray casting. Similar experiments were performed with real data using a set of 62 us images of a gall bladder. The results are shown in Figs. 4. The reconstructed cross sections show a close similarity with the observed images, except for the blurring effect which occurs at the transitions. In this case, there is no ground truth to compute the SNR as we did before. The 3D reconstruction of the organ surface obtained by thresholding and ray casting is shown in Fig. 4g-h).

5. CONCLUSION

An algorithm for 3D reconstruction of organs from a sequence of ultrasound images is described. It is assumed that the probe position and orientation are known, e.g., obtained using a electromagnetic location system. The proposed algorithm retrieves the spatial distribution of the tissue reflectivity by filtering and interpolating the available data points.

The tissue reflectivity is approximated by a linear combination of basis functions defined on a set $\Omega \subset R^3$. Since the basis functions are known only, the coefficients have to be estimated. The estimation of the unknown coefficients is performed in a Bayesian framework assuming a Rayleigh distribution for the observations and a Gibbs prior for the unknown coefficients. The use of the Rayleigh model is suggested by physical considerations about the image formation process and by the multiplicative type of noise observed in ultrasound images (speckle). The reconstruction algorithm was tested using synthetic and real data. The synthetic data consists of cross sections of a cube and the real data is a set of ultrasound images of a gall bladder obtained during a medical exam. Good results were achieved in both cases.

Acknowledgment

The ultrasound images were provided by the University of Cambridge.

6. REFERENCES

[1] J. Quistgaard, Signal Acquisition and Processing in Medical Diagnostics Ultrasound, IEEE Signal Processing Magazine, vol14, n1, pp 67-74, 1997.

[2] T. Nelson, D. Downey, D. Pretorius, A. Fenster, Three-Dimensional Ultrasound, Lippincott, 1999.

[3] T.R.Nelson, D.H.Pretorius, Interactive Acquisition, Analysis and Visualization of Sonographic Volume Data, International Journal of Imaging Systems and Technology, vol.8, pp.26-37, 1997

[4] S. Ogawa et al., Three Dimension Ultrasonic Imaging for Diagnosis of Beast Tumor,Ultrasonics Symp., 1998.

[5] R.Rohling and A. Gee, Issues in 3-D Free-Hand Medical Ultrasound Imaging, Cambridge University, 1996.

[6] C. Burckhardt, Speckle in Ultrasound B-Mode Scans, IEEE Trans. on Sonics and Ultrsonics, 25, n1, 1978.

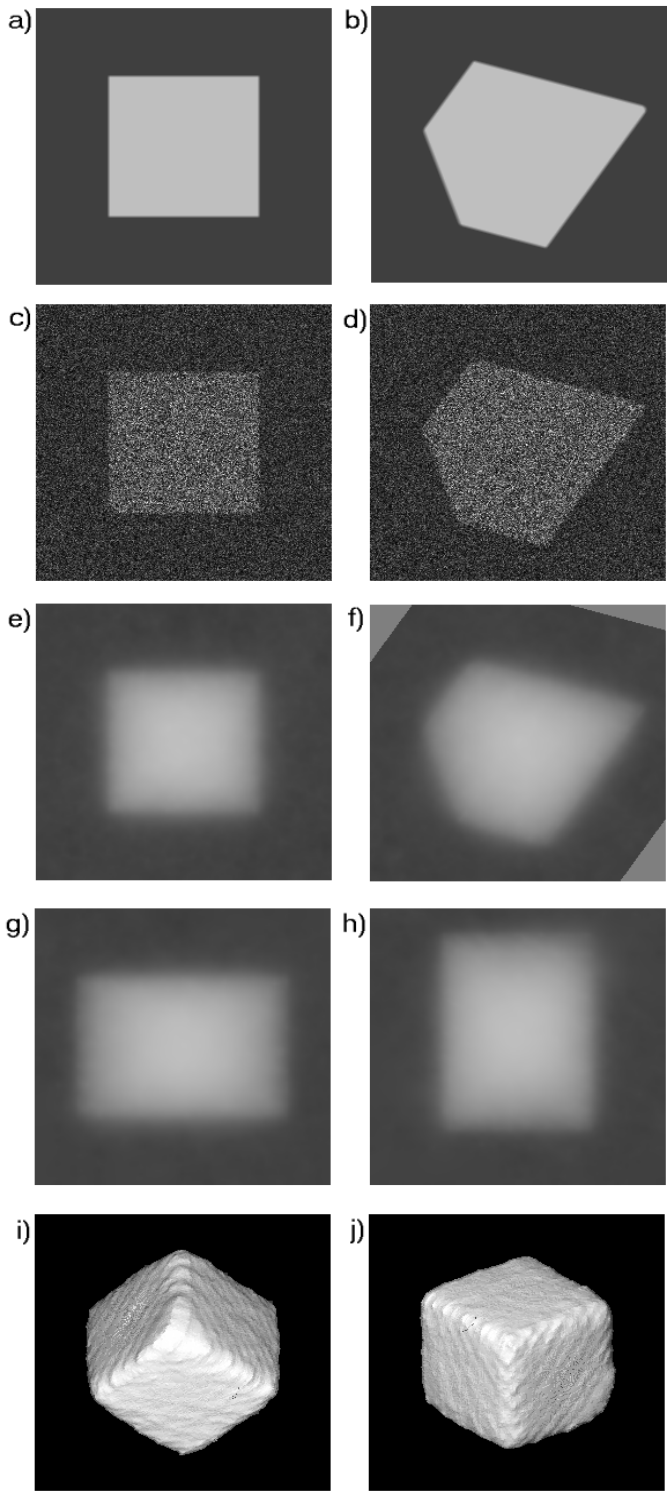

Figure 3: a-b)True planes without noise, c-d)planes with Rayleigh noise, e-f)reconstructed planes, g-h)new planes obtained from reconstructed volume, i-j) 3D reconstruction of the cube

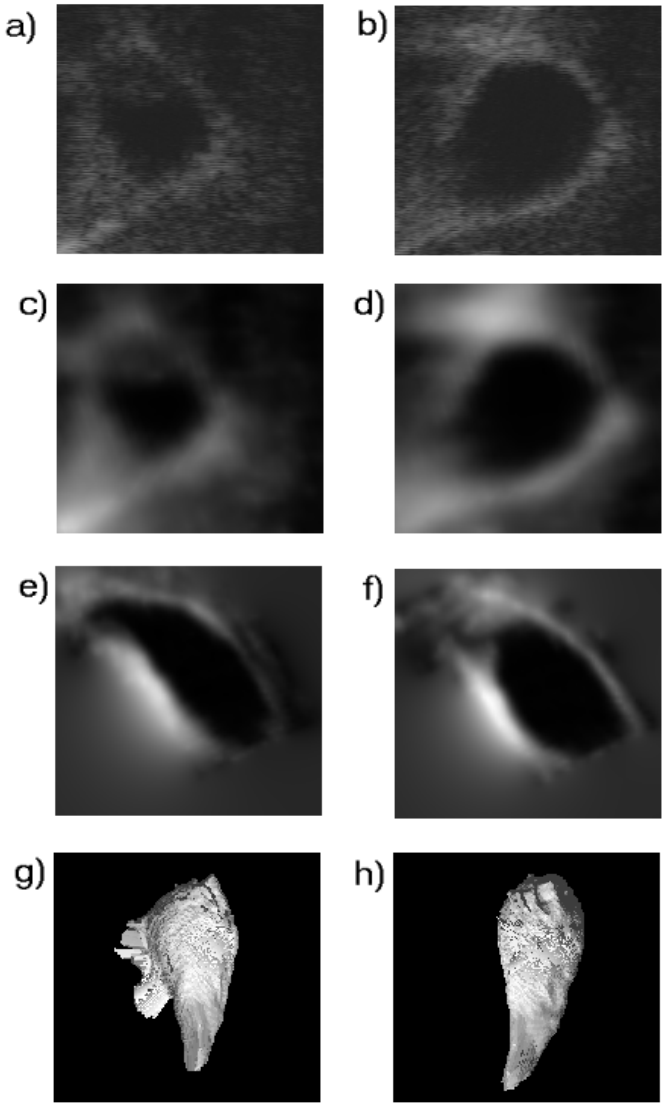

Figure 4: a-b) ultrasound images of a gall bladder, c-d) reconstructed planes; e-f) new planes of the reconstructed volume, g-h) 3D reconstruction of the gall bladder

[7] J. Abbot and F. Thurstone, Acoustic Speckle: Theory and Experimental Analysis, Ultrasound Imaging 1, 303-324, 1979.

[8] Jonathan Carr, Surface Reconstruction in 3D Medical Imaging, Ph D. Thesis, University of Canterbury, Christchurch, New Zealand, February 1996.

[9] S. Geman and D. Geman, Stochastic Relaxation, Gibbs Distributions, and the Bayesian Restoration of Images, Trans. PAMI, 6, 1984.

[10] Besag, On the Statistical Analysis of Dirty Pictures, J. R. Statist. Soc. B(1986), 48, N 3, pp. 259-302.

[11] T.A. Gooley, H.H. Barret, Evaluation of Statistical Methods of Image Reconstruction Trough ROC Analysis, IEEE Trans. on Medical Imaging, vol.11, no.2, pp.276-283, June 1992

[12] P. Shankar, Speckle Redution in Ultrasound B-Scans using Weighted Averaging in Spatial Compounding, Trans. UFFC, 33, 1986.

[13] C. Dorai, G. Wang, A. Jain, C. Mercer, Registration and Integration of Multiple Object Views for 3D Model Construction, Trans. PAMI, 83-89, 1998.

[14] W.H.Press, W.T.Vetterling, S.A.Teukolsky and B.P.Flanner, Numerical Recipes in C, Cambridge University Press, 1994

[15] G.T.Herman, A.Kuba, Discrete Tomography, Foundations, Algorithms, and Applications, Birkhauser, 1999.